Electronic Supplementary Material (ESI) for Biomaterials Science.
This journal is © The Royal Society of Chemistry 2023

Electronic Supplementary Information

Nitric oxide-releasing poly(ionic liquid)-based microneedle for subcutaneous fungal infection treatment

Qiuyang Zhang, Zijun Zhang, Xiuyang Zou, Ziyang Liu, Qingning Li, Jiamei Zhou, Shuna Gao, Hui Xu, Jiangna Guo and Feng Yan**

Jiangsu Engineering Laboratory of Novel Functional Polymeric Materials, Jiangsu Key Laboratory of Advanced Negative Carbon Technologies College of Chemistry, Suzhou Key Laboratory of Soft Material and New Energy, College of Chemistry, Chemical Engineering and Materials Science, Soochow University, Suzhou, 215123, China.

E-mail: guojn@suda.edu.cn, fyan@suda.edu.cn

Materials

2-Bromoethanol, 1-vinylimidazolium, ethyl acetate, diethyl ether, 3-amino-1-propanesulfonic acid, sodium hydroxide, azobis-(isobutyronitrile) (AIBN), DMF, petroleum ether, poly(ethylene glycol) diacrylate (PEGDA600), 1-hydroxycyclohexyl phenyl ketone (HCPK, 98%), hydroxyethyl acrylate (HEA), propidium iodide (PI), sulfanilamide, glacial acetic acid, naphthyl ethylenediamine dihydrochloride, crystal violet, β-1,3-glucanase, 2-mercaptoethanol, Tris-Cl, paraformaldehyde, calcofluor white 28 (CFW 28), 1,6-diphenyl-1,3,5-hexatriene (DPH), Triton, and 3-(4,5-dimethylthiazole-2-yl)-2,5-diphenyltetrabromazole

(MTT) were obtained from R&D Systems. Yeast extract peptone dextrose medium (YPD) and minimum essential medium (MEM) were purchased from Biosharp. *Candida albicans* (*C. albicans*, ATCC 76615) strains were used as model microorganisms. SYTO 9 green fluorescent nucleic acid stain dye was purchased from Thermo Fisher Scientific. Carboxyfluorescein diacetate, succinimidyl ester (cFDA-SE), 3-amino, 4-aminomethyl-2',7'-difluorescein, diacetate (DAF-FM DA), mouse TNF-α ELISA kit, mouse IL-1β ELISA kit and mouse IL-6 ELISA kit were purchased from Sigma-Aldrich. Mouse fibroblast cells (L929) and NIH 3T3 cells were provided by the College of Nano Science & Technology, Soochow University. All reagents were analytic grade and used as received without further purification. The water used was deionized throughout the experiments.

Characterization

^{1}H NMR spectra of the synthesized compounds were recorded on a Varian 300 MHz spectrometer using D_2O as solvent. ^{13}C NMR spectra of the synthesized compounds were recorded on a BRUKER AVANCE NEO 400 MHz. Fourier transform infrared (FT-IR) spectra were obtained on a Nicolet 5200 model spectrometer in the range of 600-4000 cm^{-1}. UV-vis absorption spectra were recorded by a TU-1800 SPC spectrophotometer. Scanning electron microscopy (SEM, Hitachi Model S-4700) was used to observe the morphology of the MNs and microbes. A fluorescence spectrometer (Cary Eclipse) was used to obtain fluorescence spectra. Fluorescence images of microbes were collected with a fluorescence microscope (Leica DM2500). The concentration of fungal suspension and hemoglobin release were recorded by a Multiskan GO microplate reader (Thermo Fisher Scientific Co). Rheological behavior tests were carried out by a RheoWin MARS 40 modular advanced rheometer. The mechanical properties were determined on an electronic tensile machine (Instron) at a speed of 0.5 mm min^{-1}. Morphology characterization of *C. albicans*

was observed by Transmission Electron Microscope HT7700 (TEM). Live/dead strain staining experiments of biofilms were measured by using a Zeiss LSM 800 laser scanning confocal microscope.

Synthesis of 3-(2-Hydroxyethyl)-1-vinylimidazolium Bromide ([HEIm][Br])

[HEIm][Br] was synthesized by stirring a mixture of an equimolar molar of 2-bromoethanol and 1-vinylimidazolium at room temperature for 48 h. The raw product was washed with ethyl acetate and diethyl ether three times and then dried at 30 °C with a rotary evaporator. ^{1}H NMR (300 MHz, D_2O, δ): 7.92-7.45 (s, 2H), 7.2-7.04 (t, 1H), 5.83 (d, 1H), 5.43 (d, 1H), 4.36 (t, 2H), 3.99 (t, 2H). ^{13}C NMR (400 MHz, D_2O): 128.35, 123.24, 119.38, 109.85, 59.68, 52.03.

Synthesis of 3-(2-Hydroxyethyl)-1-vinylimidazolium 3-Amino-1-propanesulfonic Acid ([HEIm][APS])

[HEIm][Br] was mixed with sodium 3-amino-1-propanesulfonic acid solution for 3 days to exchange the Br^- anion to 3-amino-1-propanesulfonic acid anion (APS^-). The resulting [HEIm][APS] was dried in a freezing drier. ^{1}H NMR (300 MHz, D_2O, δ): 7.87-7.44 (s, 2H), 7.19-7.06 (t, 1H), 5.80 (d, 1H), 5.43 (d, 1H), 4.37 (t, 2H), 3.97 (t, 2H), 2.93 (t, 2H), 2.76 (t, 2H), 1.88 (m, 2H). ^{13}C NMR (400 MHz, D_2O): 128.22, 123.07, 119.38, 109.57, 59.4, 51.82, 48.34, 38.88, 25.31.

Synthesis of Imidazolium-based Poly(ionic liquid)s (PIL) and NO-releasing Imidazolium-based Poly(ionic liquid)s (PIL-NO)

Poly[HEIm][APS] was synthesized by stirring a mixture containing [HEIm][APS] and AIBN (as initiator) in DMF at 60 °C for 6 h. The product was washed with acetone to remove the impurities before being further freeze-dried. The poly[HEIm][APS] was denoted as PIL. The PIL-NONOates (PIL-NO) were further

prepared by bubbling atmospheric NO into an N_2-filled sealing system with PIL. After exposure of PIL in NO for 4 h, PIL-NO was obtained.

Preparation of Poly[HEIm][APS]-based Microneedles (PILMN) and NO-releasing Poly[HEIm][APS]-based Microneedles (PILMN-NO)

A polydimethylsiloxane (PDMS) microneedle mold (12 × 12 arrays with 720 μm needle heights, 320 μm base diameter and 680 μm tip interspace) was used to fabricate the PILMN. A mixed solution containing [HEIm][APS] (30 mol %), hydroxyethyl acrylate (HEA, 70 mol %), HCPK (photoinitiator, 1 wt % of the total weight) and PEGDA (2.5 wt % of the total weight) was ultrasonicated for 30 min. Then, 40 wt % of the mixed aqueous solution was ultrasonicated into a homogeneous solution, dripped into the mold and degassed under vacuum for 30 min at room temperature to confirm that the needle tips were filled. Afterwards, the PILMN was obtained by polymerizing the mixture solution under UV irradiation (λ = 365 nm) for 30 min. The PILMN was then demolded and dried under vacuum at room temperature for 24 h before use. The PILMN-NO was further prepared by bubbling atmospheric NO into an N_2-filled sealing system with PILMN and reacted for 4 h. The amount of NO absorbed was determined at regular intervals by an electronic balance with an accuracy of ±0.0001 g. In addition, PILMN-NO with different contents of [HEIm][APS] was also synthesized and denoted as $PILMN_x$-NO (x=10, 20), where x indicated the molar ratio of [HEIm][APS].

Quantum Chemical Calculations

Gaussian 16 package was used for quantum chemical calculations [1]. Frequency calculations and geometry optimizations were performed with the solvation model based on density (water) at the M062x/6-

311++G (d, p) level. There was no imaginary frequency to ensure that each stationary point was confirmed. A self-consistent reaction field was used to perform the IR and NMR calculations using the SMD (water) model at the M062x/6-311++G (d, p) level.

Mechanical Property Characterization

The mechanical strength of MNs is important for inserting MNs into the skin. Rheological behavior tests were carried out by a RheoWin MARS 40 modular advanced rheometer with a 25 mm parallel plate. The mechanical properties of the MNs were measured with an Instron 6800 mechanical tester. Eight layers of sealing film (127 μm each layer) instead of skin were fixed on the stainless-steel surface, and the tips of MN were axially pressed at a constant rate of 0.1 mm min^{-1} [2]. The compression force was further measured for the movement of the probe as a displacement function. The MN patches placed on a horizontal table with needle tips were pointed toward the horizontal table, which gradually descended. Once the two touched, the pressure data within 600 μm were recorded.

Skin Insertion Test *In Vitro*

To test the *in vitro* skin insertion ability of PILMN-NO, PILMN-NO was inserted into fresh rabbit cadaver skin. After the MN was removed, the pinholes marked on the surface of fresh rabbit cadaver skin were imaged [3]. Afterwards, the skin was sectioned and observed with a fluorescence microscope to image the micropore structure.

NO Release of PILMN-NO *In Vitro*

PILMN-NO was soaked in 20 mL oxygen-free PBS (pH = 7.4) at 37 °C, and then a 500 μL solution

sample was taken out every 10 min. Each sample was mixed with 1 mL Griess reagent A (0.33% sulfanilamide in 20% glacial acetic acid) for diazotization. After 5 min, 1 mL Griess reagent B (0.1% naphthyl ethylenediamine dihydrochloride) was further added and incubated at room temperature for 30 min. The mixed solution was diluted to measure with UV–vis spectrometry to record the adsorption values at 540 nm to determine the NO concentration [4,5]. A similar method was used to evaluate the NO release of PIL-NO.

Transdermal NO Release of PILMN-NO *Ex Vitro*

To evaluate the transdermal NO release properties of PILMN-NO, the PILMN-NO patches were applied to fresh skin with a 500-600 μm thickness, followed by fixation to a transdermal diffusion apparatus filled with 37 °C PBS solution (pH = 7.4, 20 mL) [6]. A 0.5 mL sample was removed from the transdermal diffusion apparatus and replaced with an equal volume of fresh PBS buffer at predetermined intervals. The samples were then mixed with Griess reagent and measured with UV–vis spectrometry to record the adsorption values at 540 nm to evaluate the released NO concentration of PILMN-NO *ex vitro*.

***In Vitro* Antifungal Activity**

C. albicans in YPD medium at 37 °C with 150 rpm shaking overnight. Afterwards, the microbial suspension (2 mL) was washed with PBS solution (pH=7.4) three times at 4000 rpm for 2 min, and the microbial precipitate was resuspended in 2 mL PBS. 200 μL microbial suspension (10^8 CFU mL^{-1}) was added to sterilized PET, PILMN and PILMN-NO and incubated at 37 °C for 2 h before spreading onto agar plates. PET and PILMN were sterilized under ultraviolet light. PILMN-NO was sterilized with ultraviolet light and exposed to a NO atmosphere. The fungal viability was calculated according to the following

equation:

$$\text{fungal viability (\%)} = \frac{N_{sample}}{N_{control}} \times 100\%$$

$N_{control}$ and N_{sample} represent the number of viable microbial colonies in the control and experimental groups, respectively. Each test was repeated at least three times.

Inhibition Zone Test

The PILMN-NO patches can release NO in a mild environment, and the released NO can inhibit microbe proliferation and kill microbes. 10 μL *C. albicans* (10^8 CFU mL^{-1}) was coated onto agar plates. PILMN and PILMN-NO patches (5 × 5 mm^2) were placed on the surface of YPD agar plates and cocultured at 37 °C for 24 h. Then, the inhibition zone was observed and recorded.

2.14. Live/Dead Microbe Staining

The microbial suspension of *C. albicans* in PBS was treated with PILMN and PILMN-NO for 2 h. Afterwards, the microbes were dyed with green SYTO 9 and red PI for 15 min, followed by centrifugation and washing with PBS three times to remove the excess dyes. The stained microbes were imaged by a fluorescence microscope using an oil-immersed 100× objective lens.

Morphological Changes in Fungi

C. albicans suspension was dropped on aseptic PET films, PILMN and PILMN-NO, and cocultured for 2 h. *C. albicans* treated with PBS were used as the control group. The *C. albicans* cells were fixed with 2.5% glutaraldehyde for 2 h before dehydrating every 10 min with 10 vol%, 30 vol%, 50 vol%, 70 vol%, 80 vol%,

90 vol%, and 100 vol% ethanol solutions. The morphological changes in *C. albicans* were observed by SEM.

Biofilm Ablation Effect *In Vitro*

A crystal violet staining assay was performed to determine the ablation effect of PILMNs on *C. albicans* biofilms by evaluating the biofilm mass. Mature *C. albicans* biofilms were obtained by incubating 200 μL of *C. albicans* suspension (10^8 CFU mL^{-1}) for 48 h at 37 °C, and then the mature *C. albicans* biofilm was treated with PILMN and PILMN-NO at 37 °C for 2 h. Afterwards, the biofilms were washed with PBS three times and treated with 95% ethanol for 15 min, followed by 0.1% crystal violet staining for 30 min. Finally, the residual biofilms after being washed with PBS three times to remove the extra dye were treated with 10% acetic acid for 15 min to elute CV. The $OD_{590\ nm}$ of the resulting solution was measured using a microplate reader (Thermo Fisher). Next, supernatants in 96-well plates were analyzed using a wavelength of 490 nm. To image the microtopography change of the biofilms, the mature biofilms treated with PILMN and PILMN-NO for 2 h were stained with green SYTO 9 and red PI and observed with a 3D scanning confocal fluorescence microscope.

β-Glucanase Sensitivity

A microplate reader was used to evaluate the solidarity of β-1,3-glucan in the *C. albicans* cell wall [7]. Briefly, log-phase *C. albicans* cells were cocultured with and PILMN-NO for 2 h before being washed with PBS. Afterwards, the *C. albicans* cells ($OD_{600\ nm}$ = 0.1) were resuspended in reaction buffer (40 mM 2-mercaptoethanol, 50 mM Tris-Cl, pH 7.0). The *C. albicans* cells were treated with a 2 U mL^{-1} stock of β-1,3-glucanase followed by measuring the absorbance at 600 nm every 20 min at 37 °C for 250 min. Cells without any treatment were used as the control group.

Chitin Estimation

C. albicans in mid log-phase was used to estimate the chitin in the cells. Chitin quantification was determined after 2 h of incubation with PILMN and PILMN-NO at 37 °C. *C. albicans* suspension (10^6 CFU mL^{-1}) after treatment was fixed with 4% paraformaldehyde solution followed by washing with PBS. Then, the cells were further stained with CFW 28 (2.5 μg mL^{-1}) for 15 min [8]. The fluorescence intensity at ex 365 nm/em 435 nm of CFW 28 was measured with a fluorescence spectrometer, and the morphology of stained cells was imaged by a fluorescence microscope using an oil-immersed 100× objective lens. *C. albicans* cells without treatment were used as the control group.

Membrane Fluidity

The plasma membrane fluidity of *C. albicans* cells treated with prepared MN was determined by fluorescence spectrometry with DPH as a membrane lipid fluorescent probe [9]. Log-phase *C. albicans* cells after treatment with PILMNs for 2 h were fixed with 0.37% formaldehyde and washed with PBS. Afterwards, the *C. albicans* cells were stained with 2 μM DPH for 30 min, and fluorescence spectra were used to measure fluorescence intensity ex 350 nm/em 430 nm. *C. albicans* cells without any treatment were used as the control group.

Esterase Activity by cFDA-SE Assay

cFDA-SE, as a cell wall and membrane permeable dye, fluoresces upon hydrolysis by esterase enzymes. The esterase activity of live microbes can be evaluated by monitoring the fluorescence change of cFDA-SE, which correlates to membrane disruption [10,11]. *C. albicans* was inoculated in YPD medium overnight and

washed with PBS three times. Then, 50 μM cFDA-SE was added to the *C. albicans* suspension (10^8 CFU mL^{-1}) and incubated at 37 °C for 20 min. Afterwards, the fungal suspension was further washed with PBS and treated with PILMN and PILMN-NO at 37 °C for 2 h. A fluorescence spectrometer was used to determine the esterase activity by measuring the fluorescence intensity at ex 488 nm/em 518 nm. The fungal suspension without any treatment was used as the control group.

Intracellular NO Detection

The properties of NO diffusion and penetration in microbe cells were further evaluated [12]. A 50 μL *C. albicans* suspension in PBS (10^8 CFU mL^{-1}) was mixed with 10 μM DAF-FM DA and cocultured with PILMN-NO. DAF-FM DA (green) fluorescence images were collected every 30 min by a Leica fluorescence microscope with a 100× objective lens.

Cytotoxicity Evaluation

A 3-(4,5-dimethylthiazol-2-yl)-2,5-diphenyltetrazolium bromide (MTT) assay was used to evaluate the cytotoxicity of PILMN and PILMN-NO against mouse fibroblast cells (L929) and NIH 3T3 cells. Briefly, L929 or NIH 3T3 cells (3×10^4 CFU mL^{-1}) were cultured with MEM in a 24-well plate for 24 h, immersed in the 24-well plate and cocultured with L929 or NIH 3T3 cells. Cells without any treatment were used as a control group. After incubation at 37 °C for 24 h, 10% MTT solution (5 mg mL^{-1} PBS) was added to the wells and further cultured at 37 °C for 4 h. Afterwards, 150 μL of DMSO was added to each well to dissolve the formazan crystals. The cell viability was evaluated by testing the optical density values with a microplate assay at 570 nm. Each test was repeated three times.

Hemolysis Assay

First, the fresh blood was centrifuged at 1500 rpm for 15 min. Then, the precipitated blood cells were washed with PBS until the supernatant was pellucid. The obtained blood cells were diluted to 2 vol%. The prepared MNs were dipped into the diluted blood cell dispersion and incubated at 37 °C for 3 h. Afterwards, 100 μL supernatant was obtained by centrifuging the treated diluted blood samples at 1500 rpm for 15 min. The OD_{576nm} of the supernatant was recorded with the microplate reader to evaluate the hemoglobin release. Blood cells treated with PBS and Triton (2%) were used as negative and positive control groups, respectively. The hemolysis ratio was calculated as follows:

$$\text{Hemolysis ratio } (\%) = \frac{OD_{sample} - OD_{negative\ control}}{OD_{positive\ control} - OD_{negative\ control}} \times 100\%$$

(OD_{sample}, $OD_{positive\ control}$ and $OD_{negative\ control}$ represent the OD values of the experimental and control groups with PBS and Triton, respectively). Each test was repeated three times.

***In Vivo* Treatment of Mice with Noninfected Open Wounds**

Male C57bl/6 mice (6 weeks old, approximately 25 g) were housed in a temperature-controlled room for 5 days before the experiment. All animal experiments were conducted in accordance with the national animal research code and approved by the Ethics Committee of Soochow University. The mice were anesthetized by intraperitoneal injection of 2% sodium pentobarbital, and two wounds approximately 8 mm in diameter were made on their shaved backs. The noninfected open wounds were locally treated with PILMN and PILMN-NO only once for two hours. Images of the wound sites of the mice were recorded by a digital camera every 2 days. After 9 days of treatment, all mice were sacrificed, and the infected tissues were excised

from the mice for ELISA.

In Vivo Treatment of C. albicans-induced Subcutaneous Abscess

Male C57bl/6 mice (6 weeks old, approximately 25 g) were housed in a temperature-controlled room for 5 days before the experiment. All animal experiments were conducted in accordance with the national animal research code and approved by the Ethics Committee of Soochow University. The mice were anesthetized by intraperitoneal injection of 2% sodium pentobarbital before injecting 100 μL *C. albicans* (10^8 CFU mL^{-1}) suspensions subcutaneously to create an abscess infection model. After 24 h, a *C. albicans* subcutaneous abscess formed. The infected mice were randomly divided into three groups with four mice in each group. The infected mice were locally treated with PILMN and PILMN-NO only once for two hours. Images of the infected sites of the mice were recorded by a digital camera every 2 days. The mice were sacrificed on the third day, and the infected site tissues were excised and ground into homogenate. Afterwards, the tissue homogenate was diluted and spread onto YPD agar plates to determine the colony number of fungi. After 11 days of treatment, all mice were sacrificed, and the infected tissues were excised from the mice for ELISA. Histology and immunohistochemistry staining (H&E staining, Masson staining and immunohistochemistry CD31 staining) of the infected tissues were used to assess the healing of abscesses *in vivo*. PBS-injected mice were used as the negative control group, and the infected mice without any treatment were classified as the positive control group.

Statistical Analysis

The experiments above were repeated at least three times. All experimental statistics are presented as the means and SD. The statistical significance was evaluated by Student's t test when only two groups were

compared.

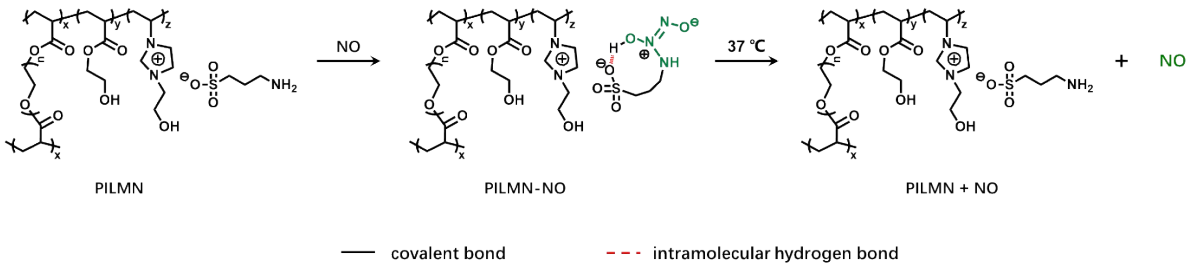

Scheme S1. The chemical structures of PILMN and PILMN-NO and NO storage/release chemistry.

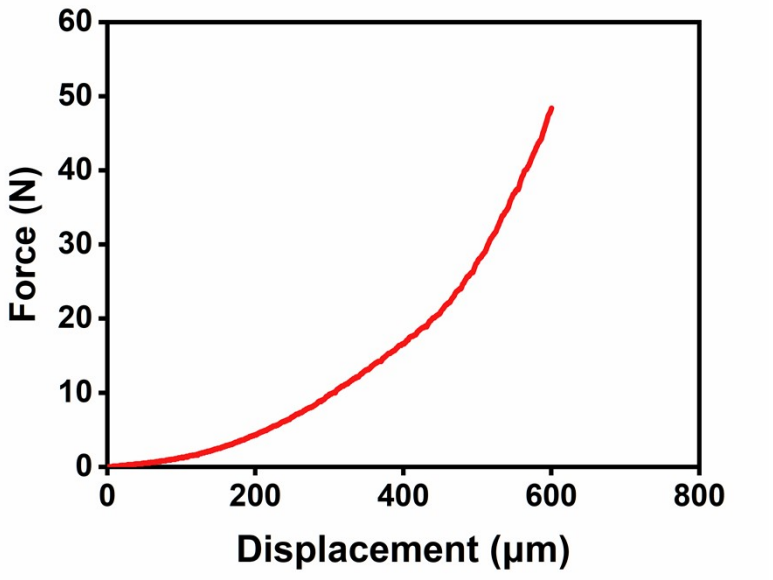

Fig. S1 Force–displacement curves of PILMN-NO recorded during penetrating eight-layer

sealing films at 400 μm after storing in NO atmosphere for 2 days.

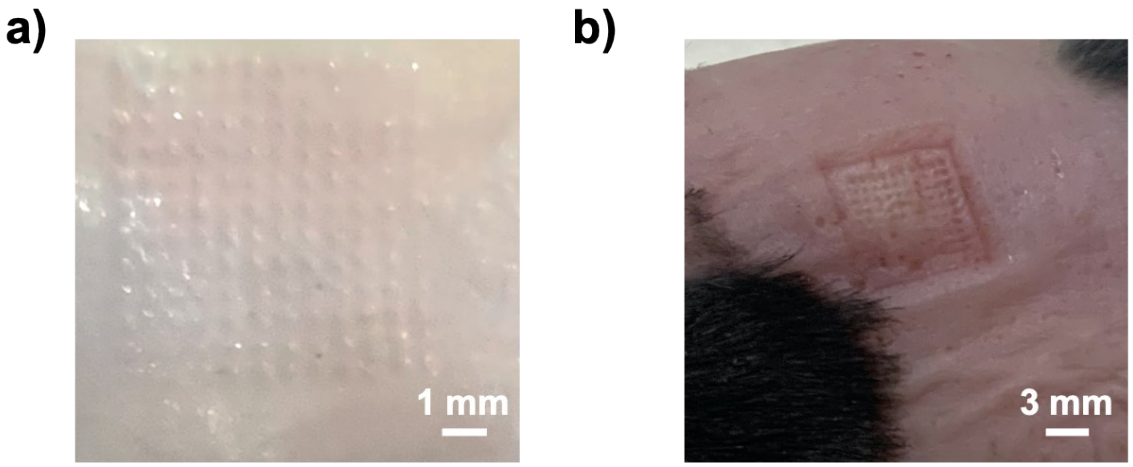

Fig. S2 Photographs of pinholes after inserting PILMN-NO into a) rabbit skin and b) live mouse skin.

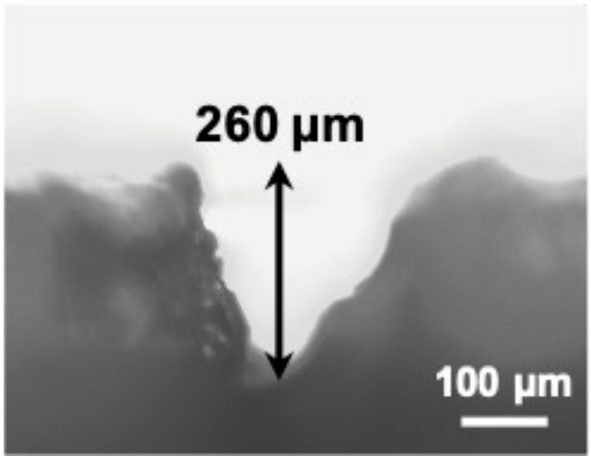

Fig. S3 Optical microscope of fresh skin after the insertion of PILMN-NO.

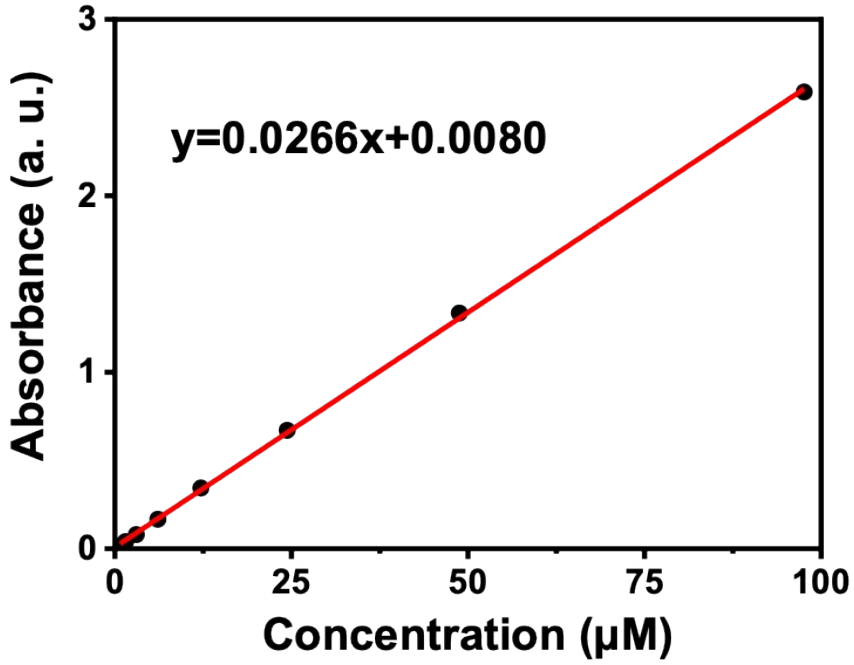

Fig. S4 Calibration curve of NO released in PBS characterized by a UV–vis spectrometer.

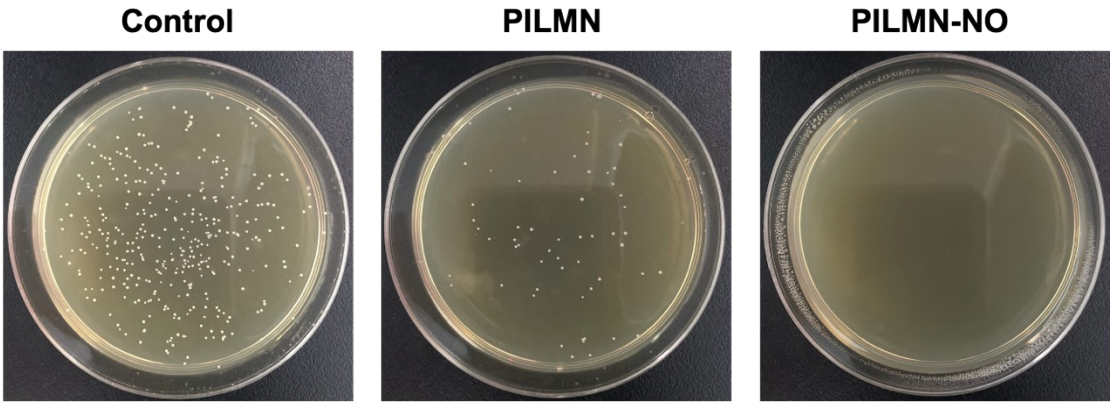

Fig. S5 Photographs of agar plates for antifungal activity of PILMN and PILMN-NO against *C. albicans in vitro*.

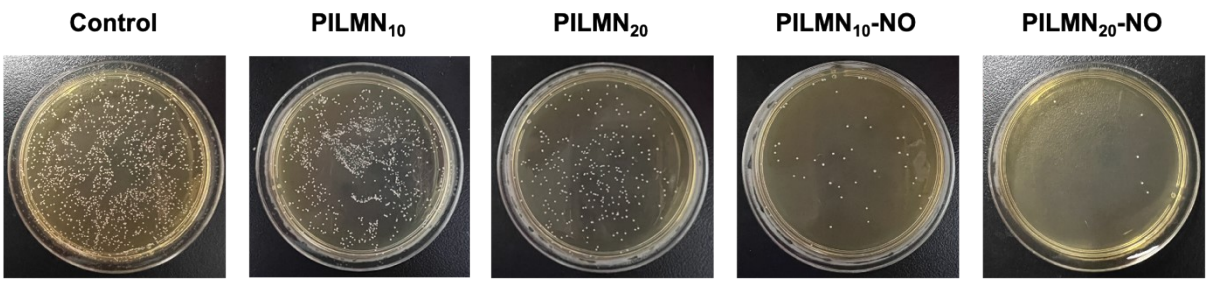

Fig. S6 Photographs of agar plates for antifungal activity of $PILMN_{10}$, $PILMN_{20}$, $PILMN_{10}$-NO, and $PILMN_{20}$-NO against *C. albicans in vitro*.

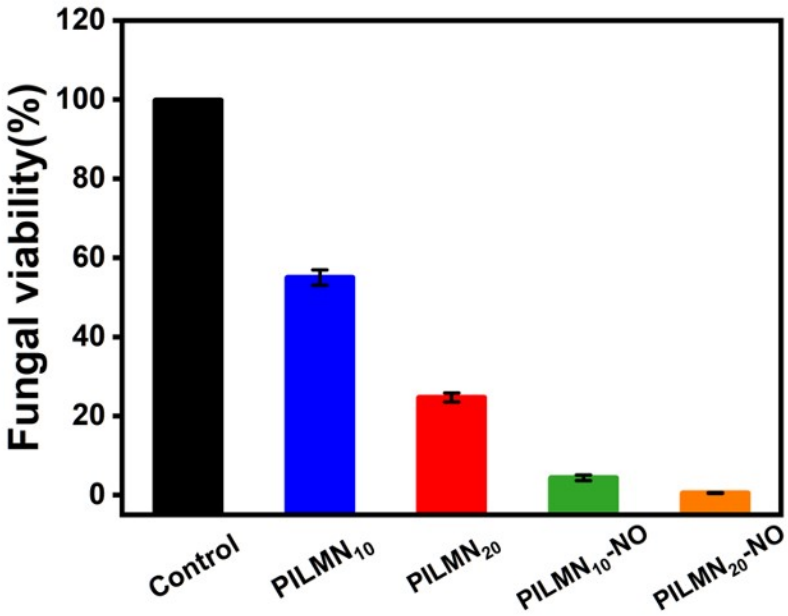

Fig. S7 Viabilities *of C. albicans* after being treated with $PILMN_{10}$, $PILMN_{20}$, $PILMN_{10}$-NO, and $PILMN_{20}$-NO for 2 h.

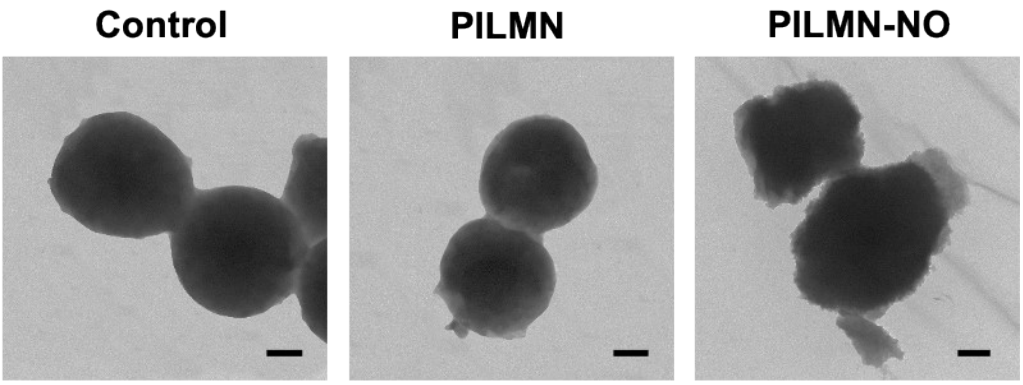

Fig. S8 TEM images of *C. albicans* with the treatment of PILMN and PILMN-NO, respectively, (scale bar: 200 nm).

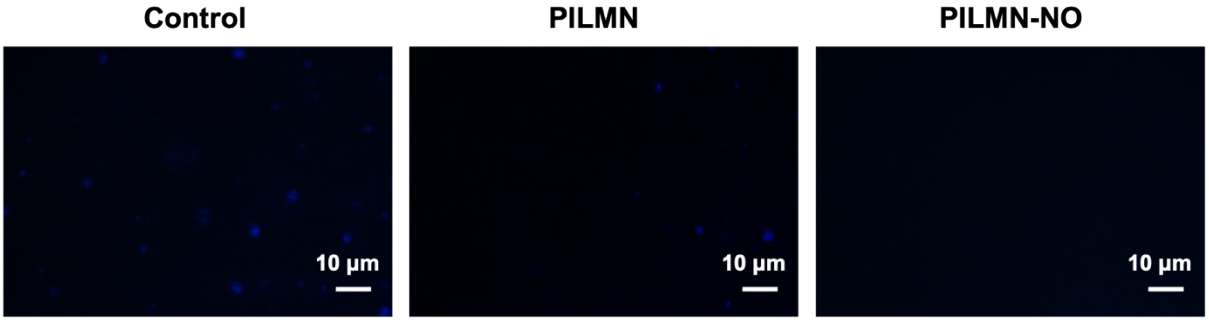

Fig. S9 Fluorescence images of chitin in *C. albicans* stained with CFW 28 after different treatments.

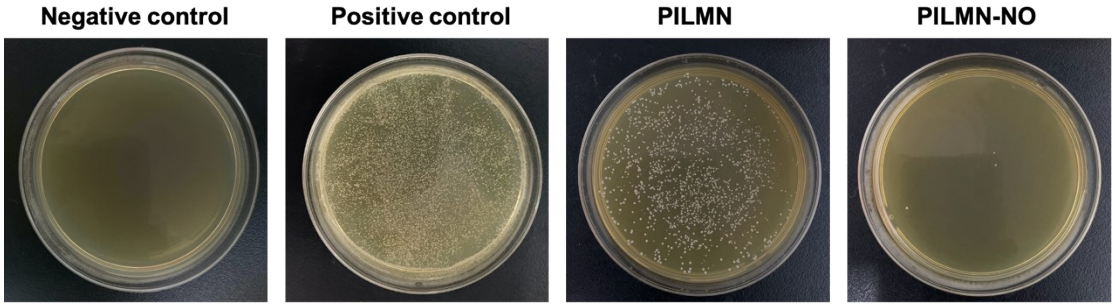

Fig. S10 Photographs of agar plates for antifungal activities of PILMN and PILMN-NO against *C. albicans* by colony counting assay *in vivo*.

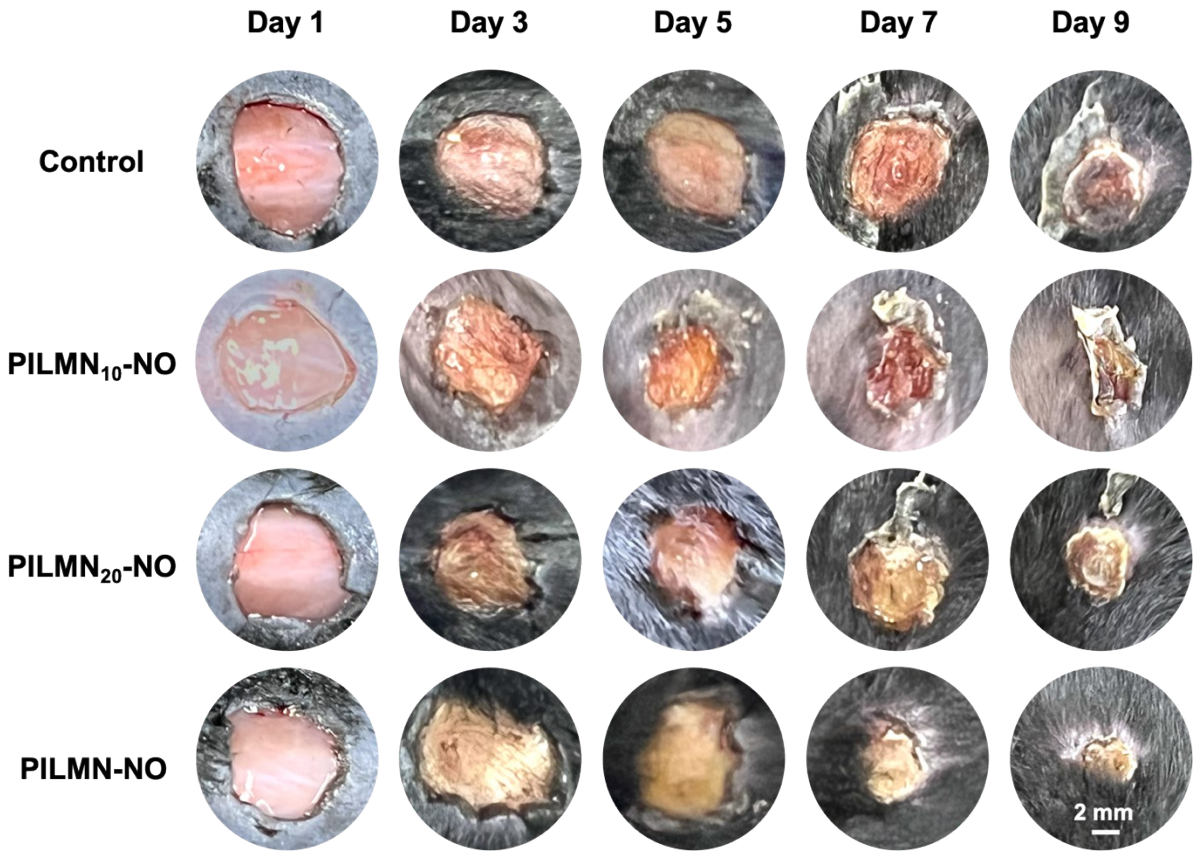

Fig. S11 Representative images of noninfected open wound in mice at day 1, 3, 5, 7 and 9 (scale bar: 2 mm).

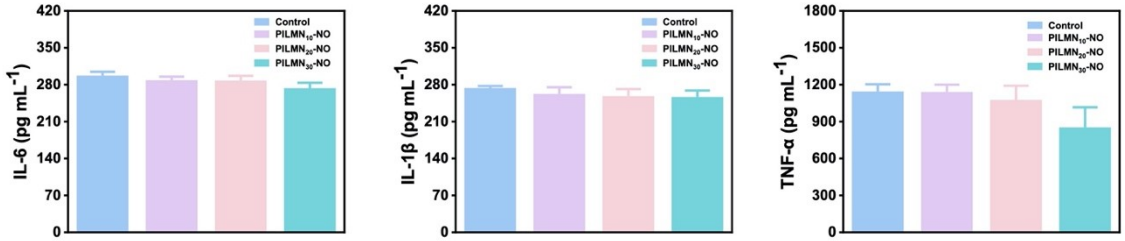

Fig. S12 Expression level (pg mL^{-1}) of IL-6, IL-1β and TNF-α of mice after different treatments on day 9.

References

1 M. J. Frisch, G. W. Trucks, H. B. Schlegel, G. E. Scuseria, M. A. Robb, J. R. Cheeseman, G. Scalmani, V. Barone, G. A. Petersson, H. Nakatsuji, X. Li, M. Caricato, A. V. Marenich, J. Bloino, B. G. Janesko, R. Gomperts, B. Mennucci, H. P. Hratchian, J. V. Ortiz, A. F. Izmaylov, J. L. Sonnenberg, D. Williams-Young, F. Ding, F. Lipparini, F. Egidi, J. Goings, B. Peng, A. Petrone, T. Henderson, D. Ranasinghe, V. G. Zakrzewski, J. Gao, N. Rega, G. Zheng, W. Liang, M. Hada, M. Ehara, K. Toyota, R. Fukuda, J. Hasegawa, M. Ishida, T. Nakajima, Y. Honda, O. Kitao, H. Nakai,T. Vreven, K. Throssell, J. A. Montgomery, Jr., J. E. Peralta, F. Ogliaro, M. J. Bearpark, J. J. Heyd, E. N. Brothers, K. N. Kudin, V. N. Staroverov, T. A. Keith, R. Kobayashi, J. Normand, K. Raghavachari, A. P. Rendell, J. C. Burant, S. S. Iyengar, J. Tomasi, M. Cossi, J. M. Millam, M. Klene, C. Adamo, R. Cammi, J. W. Ochterski, R. L. Martin, K. Morokuma, O. Farkas, J. B. Foresman, and D. J. Fox, Gaussian, Inc., Wallingford CT, 2016.

2 M. Zhu, Y. Liu, F. Jiang, J. Cao, S. C. Kundu and S. Lu, *ACS Biomater. Sci. Eng.,* 2020, **6**, 3422–3429.

3 H. Yang, X. Wu, Z. Zhou, X. Chen and M. Kong, *Int. J. Biol. Macromol.,* 2019, **125**, 9–16.

4 Z. Yuan, C. Lin, Y. He, B. Tao, M. Chen, J. Zhang, P. Liu, K. Cai, *ACS Nano,* 2020, **14**, 3546–3562.

5 S. Paul, S. Pan, A. Chakraborty, P. De and A. Mukherjee, *ACS Appl. Polym. Mater.,* 2021, **3**, 2310–2315.

6 C. Fang, L. Kong, Q. Ge, W. Zhang, X. Zhou, L. Zhang and X. Wang, *Polym. Chem.,* 2019, **10**, 209–218.

7 A. Burgain, F. Tebbji, I. Khemiri and A. Sellam, *mSphere,* 2020, **5**. E00913-19.

8 P. Gupta and K. M. Poluri, *ACS Bio Med Chem Au,* 2022. **2**. 60-72.

9 A. Bhattacharyya, M. Sinha, H. Singh, R. S. Patel, S. Ghosh, K. Sardana, S. Ghosh and S. Sengupta, *Front. Microbiol.,* 2020, **11**, 2116.

10 R. Kannan, P. Prabakaran, R. Basu, C. Pindi, S. Senapati, V. Muthuvijayan and E. Prasad, *ACS Appl. Bio Mater.,* 2019, **2**, 3212–3224.

11 Z. Zhou, C. Ergene, J. Y. Lee, D. J. Shirley, B. R. Carone, G. A. Caputo and E. F. Palermo, *ACS Appl. Mater. Interfaces,* 2019, **11**, 1896–1906.

12 L. Yang and M. H. Schoenfisch, *ACS Appl. Bio Mater.,* 2018, **1**, 1066–1073.